frontiers | Frontiers in Earth Science

TYPE Original Research
PUBLISHED 30 January 2023
DOI 10.3389/feart.2022.987349

OPEN ACCESS

EDITED BY
Andrea Taschetto,
University of New South Wales, Australia

REVIEWED BY
Cheng Sun,
Beijing Normal University, China
Botao Zhou,
Nanjing University of Information Science and Technology, China
Sang-Wook Yeh,
Hanyang University, South Korea

*CORRESPONDENCE
Dong Xiao,
xiaodong1981@foxmail.com

SPECIALTY SECTION
This article was submitted to Atmospheric Science, a section of the journal Frontiers in Earth Science

RECEIVED 06 July 2022
ACCEPTED 05 December 2022
PUBLISHED 30 January 2023

CITATION
Xiao D and Ren H-L (2023), A regime shift in North Pacific annual mean sea surface temperature in 2013/14. *Front. Earth Sci.* 10:987349. doi: 10.3389/feart.2022.987349

A regime shift in North Pacific annual mean sea surface temperature in 2013/14

Dong Xiao [1,2]* and Hong-Li Ren[2]

[1]Key Laboratory of Cities' Mitigation and Adaptation to Climate Change in Shanghai, China Meteorological Administration, Shanghai, China, [2]State Key Laboratory of Severe Weather, Chinese Academy of Meteorological Sciences, Beijing, China

This study revealed a new regime shift in the North Pacific annual mean sea surface temperature (SST) in 2013/14, robust in multiple SST data sets. This regime shift shows a horseshoe pattern with warming SST along the North American western coast and toward the Central Pacific. It suggests a phase reversal of the Victoria Mode (VM) and it seems unrelated to the shift in the Pacific Decadal Oscillation (PDO) and Interdecadal Pacific Oscillation (IPO). Associated with this regime shift, the annual surface air temperature significantly enhanced over the high-latitude landmass after 2014, whereas it declined over northeastern Canada and southwestern Greenland. The annual precipitation generally increased (decreased) in the Northern (Southern) Hemisphere landmass monsoon regions. There are no regime shifts in Equatorial Central-East Pacific SST and the intensity and locations of the Aleutian Low around 2013/14. These facts suggest the regime shift of North Pacific SST in 2013/14 may not originate from the decadal variations of the midlatitude atmosphere and tropical ocean. The extensive influence of this regime shift in 2013/14 on the atmospheric, oceanic and ecological systems warrants further investigation.

KEYWORDS

regime shift, sea surface temperature, Pacific decadal oscillation, Victoria mode, Aleutian low

Introduction

During the past century, the North Pacific Sea Surface Temperature (SST) experienced several regime shifts also called decadal abrupt changes (DACs). These include the transition to the positive phase of the Pacific Decadal Oscillation (PDO) with a warming horseshoe pattern in the North Pacific SST in 1924/25 (Mantua et al., 1997; Xiao and Li, 2007a), the warming regime shift of central North Pacific SST (Xiao and Li, 2007a) and the transition to negative phase of PDO (Mantua et al., 1997; Zhang et al., 1997) in approximately 1941/42, the well-known regime shift to positive phase of PDO in 1976/77 with cooler SST in central North Pacific, and the opposite in other regions of the North Pacific and deeper Aleutian Low (Nitta and Yamada, 1989; Trenberth, 1990; Mantua et al., 1997; Minobe, 1997; Zhang et al., 1997; Power et al., 1999; Hare and Mantua, 2000; Mantua and Hare, 2002; Wu et al., 2005; Xiao and Li, 2007b), warmer SST over the

northern north Pacific SST in l988/89 (Hare and Mantua, 2000; Yeh et al., 2011; Xiao et al., 2012; Jo et al., 2013; Song et al., 2020), and a recent transition to negative phase of the PDO in 1997/98 (Xiao and Li, 2007a; Hong et al., 2014; Doi et al., 2015; Dong and Dai, 2015; Jo et al., 2015; Zhu et al., 2015; Ellis and Marston, 2020; You et al., 2021). The regime shifts in the North Pacific SST during the past century remarkably influenced the atmospheric circulation, and marine and terrestrial ecosystems (Mantua et al., 1997; Mantua and Hare, 2002; Chavez et al., 2003). It is worth paying more attention to the regime shifts in the North Pacific SST.

The PDO is defined by the leading empirical orthogonal function (EOF1) mode of monthly SST anomalies (SSTA, deviation from the climatological cycle) in the North Pacific north of 20°N (Mantua et al., 1997). The spatial pattern of the PDO resembles a horseshoe with SST anomalies over the central North Pacific SST surrounded by opposite SST anomalies toward North America and the Topics. Decadal variations of SST are not confined to the North Pacific but also appear in the whole Pacific. The Interdecadal Pacific Oscillation (IPO) displays a pattern with identical anomalies in the central North and South Pacific and opposite anomalies in the Central-East Pacific (Power et al., 1999). The IPO index is defined as the difference between the SSTA averaged in the central-eastern Pacific and the average of SSTA in the South and North Pacific regions (Henley et al., 2015). Although the mechanisms of PDO and IPO are still unclear, they show high consistency on decadal and interdecadal time scales (Han et al., 2014). The PDO and IPO both changed phases in 1924/25, 1941/42, 1976/77, and 1997/98 (Mantua et al., 1997; Power et al., 1999; Henley et al., 2015). The temporal evolution of the PDO and IPO and their associated atmospheric circulation anomalies have attracted much attention because of their relationship to the Pacific ecosystem (Francis and Hare, 1994; Mantua et al., 1997; Hare and Mantua, 2000; Mantua and Hare, 2002; Chavez et al., 2003), North American precipitation, jet stream (intensity and location) and air temperature (Cayan et al., 1998; Deser et al., 1999; Mantua and Hare, 2002; Mochizukia et al., 2010), East-Asian precipitation and drought (Zhu et al., 2015; Li et al., 2017; Qin et al., 2018; Yao et al., 2018; Lee et al., 2019; Wang et al., 2019), South China Sea summer monsoon (Wu and Mao, 2017; Xu et al., 2021), global precipitation extreme (Wei et al., 2021), fluctuations of Asian monsoon (Krishnan and Sugi, 2003), Australian climate (Power et al., 1999; Doi et al., 2015) and modulation on El Niño-Southern Oscillation (ENSO) (Newman et al., 2003; Alexander et al., 2008; Hu and Huang, 2009; Newman et al., 2016).

The PDO alone cannot fully characterize the climate variability over the North Pacific. In recent years, there has been an increasing number of studies paying attention to the second mode of the North Pacific SSTA. The Victoria mode (VM) is defined as the second EOF mode (EOF2) of the North Pacific SSTA poleward of 20°N (Bond et al., 2003). Distinguished from the PDO, the positive phase of VM displays positive anomalies poleward of 35°N and eastward of 160°W with the center over the northeastern Pacific and negative anomalies over the other regions with the center in the intersection between the northern subtropical Central Pacific and the dateline. Such a northeast-southwest-oriented SSTA dipole pattern shows significant interannual and interdecadal variability (Ding et al., 2015a). The temporal variability of the VM index has a significant influence on the surrounding Pacific climate, including the Pacific Intertropical Convergence Zone (ITCZ) precipitation (Ding et al., 2015a), the anticyclone over the western North Pacific, and the winter rainfall over South China (Zou et al., 2020) and the western North Pacific tropical cyclone frequency (Pu et al., 2018). It can also be the linkage between North Pacific Gyre Oscillation and ENSO (Ding et al., 2015b) and contribute to the development and propagation of the Madden-Julian Oscillation (Wen et al., 2020).

There are two significant periodicities in the North Pacific SST, one of 15–25 years and the other of 50–70 years (Minobe, 1997; Hare and Mantua, 2000; Minobe, 2000). More than 20 years have passed since the regime shift in 1997/98. One concern is whether a new regime shift has recently occurred in the Pacific SST. If it exists, there would be a wide application of the climate variability and prediction associated with the regime shift. Therefore, we posed the following questions: Has a new regime shift occurred in North Pacific SST recently? Has the leading and second mode of the North Pacific SST (PDO and VM) experienced a regime shift recently? Is there any difference between this regime shift and the previous one? Has precipitation and temperature significantly changed after this regime shift? What is the possible cause of this regime shift? With these questions in mind, we examined the regime shifts in the Pacific SST by using a moving *t*-test technique. A new regime shift in the North Pacific SST was found in 2013/14. We detected whether this regime shift occurred in the PDO and VM indexes and compared the difference in SST between the regime shifts in 2013/14 and 1976/77. The changes in temperature and precipitation over the landmass before and after this regime shift are investigated. The possible causes of this regime shift are discussed from extratropical and tropical views.

Data and methodology

This study employed four global observational monthly SST data sets, including the fifth version of Extended Reconstructed SST (ERSST5) (Huang et al., 2017), Hadley Centre Sea Ice and SST (HadISST) (Rayner et al., 2003), the Centennial *in situ* Observation-Based Estimates (COBE) SST (Ishii et al., 2005), and the Kaplan SSTA (Kaplan et al., 1998). The resolutions of above SST data sets are 2° × 2°, 1° × 1°, 1° × 1°, and 5° × 5°, respectively. Their common periods of 1900–2021 were focused on in this study. The landmass monthly precipitation and Surface Air Temperature are available from Climate Research Unit

(CRU) and gridded at a resolution of 0.5° × 0.5° for the period from January 1900 to December 2021 (Harris et al., 2020). We obtained the monthly mean sea level pressure (SLP) from the fifth generation of European Centre for Medium-Range Weather Forecasts (ECMWF) Reanalysis (ERA5) (https://cds.climate.copernicus.eu) (Hersbach et al., 2020). These are global, gridded data at a resolution of 0.75° × 0.75° for the period from January 1950 to February 2022. The monthly PDO and VM indexes, which are defined as the leading and second EOF modes of the North Pacific SSTA north of 20°N (Mantua et al., 1997; Bond et al., 2003) using SST data sets of ERSST5, HadISST, and COBE SST, respectively, are available from National Oceanic and Atmospheric Administration (NOAA) Physical Sciences Laboratory (PSL) (https://psl.noaa.gov/pdo/) and homepage of Prof. Ding Rui-Qiang (http://staff.lasg.ac.cn/drq/index/download), respectively.

In modern climate change studies, the regime shift is generally defined as a rapid transition from a mean climate state to another one (Rodionov, 2004; Overland et al., 2008). The rapid transition period is generally one time-unit (1 year in this study) or between two time-units (such as 2013/14 between 2013 and 2014), much shorter than the duration of the mean state, which is considered here as the mean value of a period of 10 years or longer. To better understand the time scale and kind of transition, Xiao and Li (2007a); Xiao and Li (2007b) called the regime shift the decadal abrupt change (DAC) of the mean value. Many detection methods were introduced and developed for searching regime shifts in time series by examining climate statistics, such as mean values or variance (Fu and Wang, 1992; Easterling and Peterson, 1995; Rodionov, 2004; Xiao and Li, 2007a; Xiao and Li 2007b; Overland et al., 2008; Reid et al., 2016), and dynamical entropy (He et al., 2012; He et al., 2013; He et al., 2015; He et al., 2016; Jin et al., 2016; Liu et al., 2017). Xiao and Li (2007a) compared the advantages and disadvantages of these current methods for examining the regime shifts. They developed a moving t-test technique method by performing the normal distribution skewness and kurtosis test, effective freedom degree correction, and multiple testing corrections to better detect DACs in the ocean and atmosphere systems (Xiao and Li, 2007b). This modified moving t-test technique can be easily applied to examine the DACs of the mean value objectively in time series (Xiao and Li 2007a; Xiao and Li, 2007b; Xiao and Li, 2011; Xiao et al., 2012; Xiao and Ren, 2021; Xiao et al., 2021).

For a time series with a sample size n (X_i, i=1, 2, ..., n), the moving t-test technique is performed by moving a cutting point before and after to get two subsets (x_1 and x_2) and then detecting the significance between them. The t-statistic is defined as follows:

$$t = \frac{\overline{x_2} - \overline{x_1}}{s \cdot \sqrt{\frac{1}{n_1} + \frac{1}{n_2}}}$$

Where $s = \sqrt{\frac{n_1 s_1^2 + n_2 s_2^2}{n_1 + n_2 - 2}}$, n_1, n_2 are the sample sizes for the subset x_1 and x_2, respectively, namely the detecting scales of the moving t-test technique. $\overline{x_1}$ and s_1^2 ($\overline{x_2}$ and s_2^2) denote the mean value and variance of the subset x_1 (x_2), respectively. Given a significant level α, the DAC year (DACY) is corresponding to the years with maximal or minimal t-values under the situation ($|t| \geq t_\alpha$). The increased (decreased) DAC denotes that the n_2-year mean value after the DACY is the most significant one among these larger (lower) than n_1-year one before the DACY. In this study, we choose $n_1 = n_2 = 10$, the approximate lower limit of the decadal time scale, to examine the DACY. The time scale equal to 10 ($n_1 = n_2 = 10$) means that the duration of the mean value between two neighbor DACYs is approximately equal to or larger than 10 years. In this study, we use both two concepts (regime shift and DAC). For example, the DACY is 2013, namely, the DAC happened in 2013. The DAC in 2013 also can be called the regime shift in 2013/14 to show the time of sudden change between the years 2013 and 2014 because the variable in 2013 (2014) belongs to the epoch average before (after) the regime shift. The epoch average (mean) is the mean value during a certain period between the neighbor DACYs (or DACY and marginal year) of a time series. For instance, there are two DACYs (1997 and 2013) in a time series from 1950 to 2021. The epoch means are the average of the time series during 1950–1997, 1998–2013, and 2014–2021.

Results

Figure 1 shows the horizontal distribution of DACYs of annual mean Pacific SST in four data sets. In ERSST5, the increased DACs of SST displayed a horseshoe shape over the North Pacific along the west coast of North America and toward the Bering Strait and Central Pacific (Figure 1A). They took place to the west of Mexico in 2011 and 2012, around Hawaii in 2012, in the northeastern North Pacific in 2011 and 2012, in other domains of the horseshoe shape in 2013, and in the gulf of Mexico in 2013 and 2014. The DACs of SST in HadISST (Figure 1B) also showed a horseshoe and occurred in most of the horseshoe region in 2013 and in the Mexico gulf and part of the Central Pacific in 2013 and 2014. The distribution of the DACYs in COBE SST (Figure 1C) is highly similar to those in ERSST5 (Figure 1A). In Kaplan SSTA (Figure 1D), the distribution of DACYs in SSTA also indicates a hoof shape with the DACs mainly happening in 2013. The distribution of DACs in ERSST5, HadISST, COBE SST, and Kaplan SSTA all showed a hoof shape over the North Pacific and mainly occurred in 2013 or 2014 (Figure 1). These results suggest that the spatial pattern of the increased DACs of SST around 2013 is robust among the four SST data sets.

The regime shift (DAC) of the mean value can be easily seen in a time series. Therefore, we divided the horseshoe region of the North Pacific into three boxes and showed their time series in four SST data sets. In each of the panels in Figure 1, Box 1, 2, and 3 stand for the northern North Pacific (170°E–120°W, 45°–65°N),

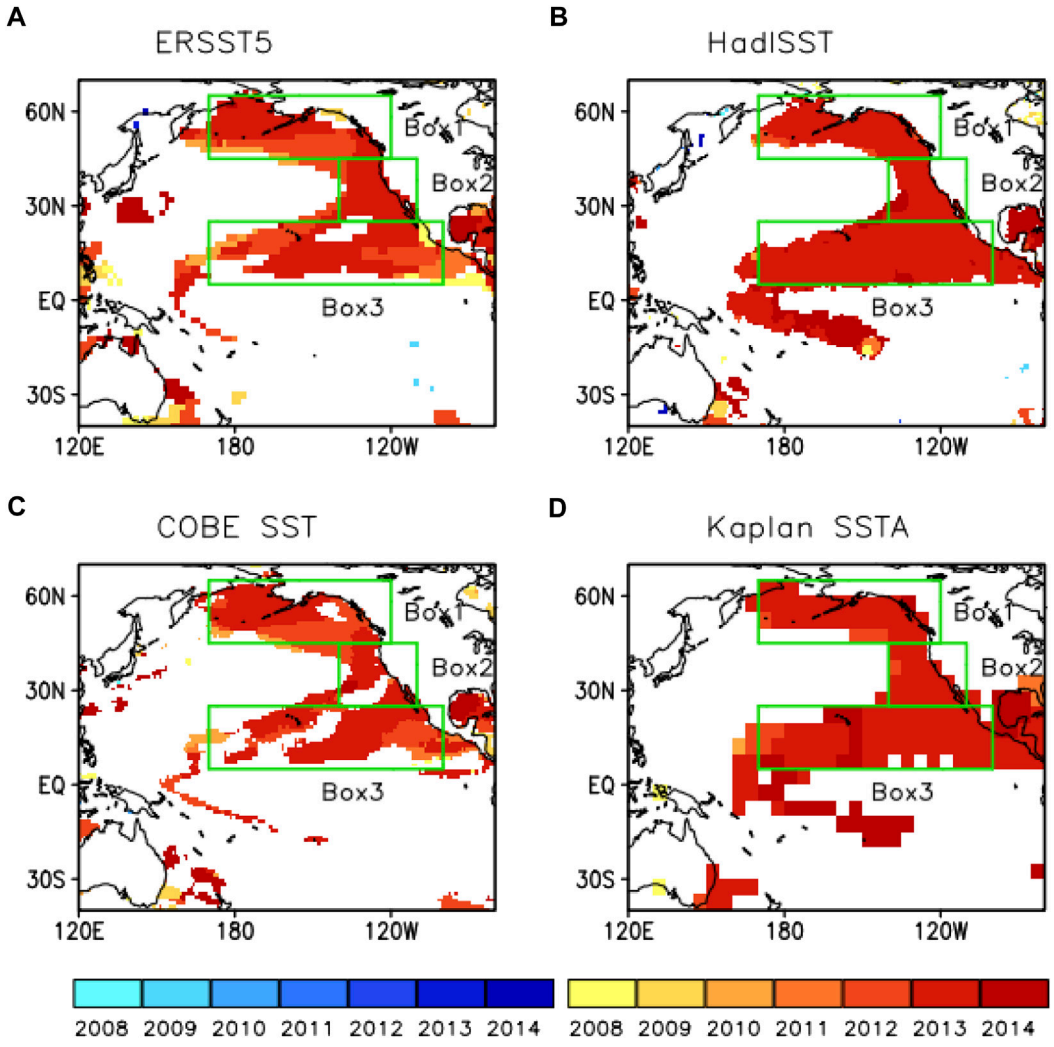

FIGURE 1
The horizontal distribution of the DACYs (shading) during 2008–2014 in **(A)** ERSST5, **(B)** HadISST, **(C)** COBE SST, and **(D)** Kaplan SSTA, which were detected by the moving *t*-test technique at the 95% confidence level. The horizontal distribution of the DACYs during 2008–2014 is the overlapped time cross-sections of the DACYs of each grid in the horizontal SST field during the same period. Warm (cold) color shading refers to the increased (decreased) DACs of SST. The green boxes from top to bottom in each panel are Box 1, Box 2, and Box 3, respectively.

the eastern North Pacific (110°W–130°W, 25°–45°N), and the northern Tropical Central and East Pacific (170°E–100°W, 5°–25°N), respectively. Figures 2A–D gives the time series of SST in Box 1 in ERSST5, HadISST, COBE SST, and Kaplan SSTA, respectively. The northern North Pacific (Box 1) SST in ERSST5 (Figure 2A) experienced two significantly increased DACs in 1977 and 2013 with the enhancements of the mean value of 0.28 °C and 0.83°C, respectively (Figure 2A). There were also two increased DACs in 1977 and 2013 in the HadISST (COBE SST and Kaplan SSTA) data set with increases of the mean value of 0.45°C (0.26°C and 0.33°C) and 0.58°C (0.71°C and 0.72°C), respectively (Figures 1B–D). Additionally, there was also a decreased DAC in 1967 in Kaplan SSTA with a decrease of the epoch mean of 0.19°C (Figure 1D). SST in Box 2 over the eastern North Pacific shows increased DACs around 1978 and 2013 and a decreased DAC in 1998 in these four SST data sets (Figures 2E–H). Compared to the previous epoch average, the increase of the epoch average after 1978 (1998) is 0.37°C (−0.38°C) in ERSST5 (Figure 2E), 0.32°C (−0.31°C) in HadISST (Figure 2F), 0.32°C (−0.33°C) in COBE SST (Figure 2G) and 0.37 °C (−0.37 °C) in Kaplan SSTA (Figure 2H). Furthermore, the mean value during 2014–2021 in ERSST5 (HadISST, COBE SST, and Kaplan SSTA) is 0.97°C (0.81°C, 0.86°C, and 0.80 °C) higher than that during 1999–2013. The northern Tropical Central Pacific SST of ERSST5 in Box 3 (Figure 2I) witnessed an increased DAC in 1979

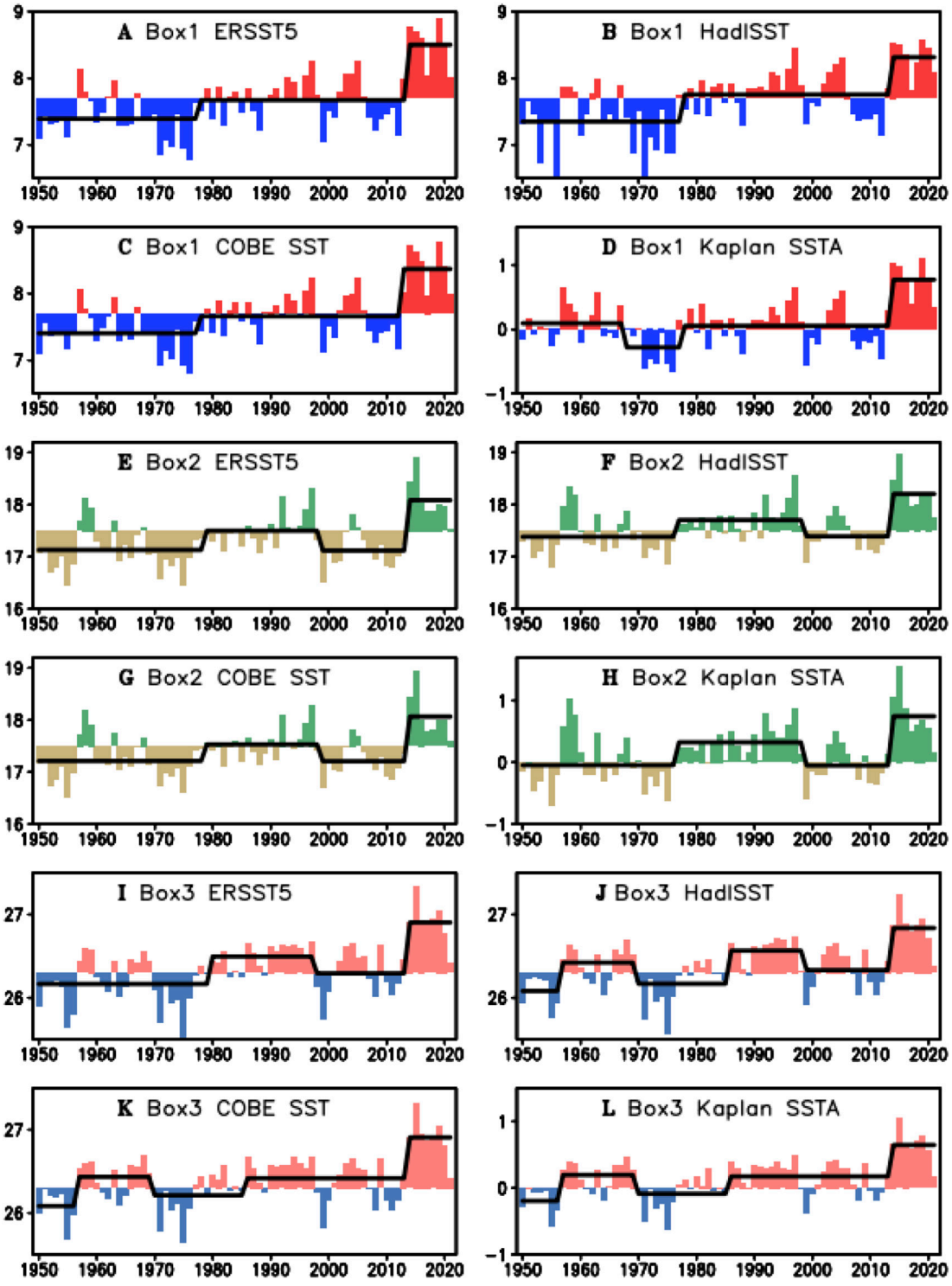

FIGURE 2
Time series (colored bar) and epoch average (black thickened solid line) of **(A–D)** Box 1, **(E–H)** Box 2, and **(I–L)** Box 3 annual mean SST in four data sets during 1950–2021. The domains of Boxes 1–3 are indicated in the corresponding panel in Figure 1.

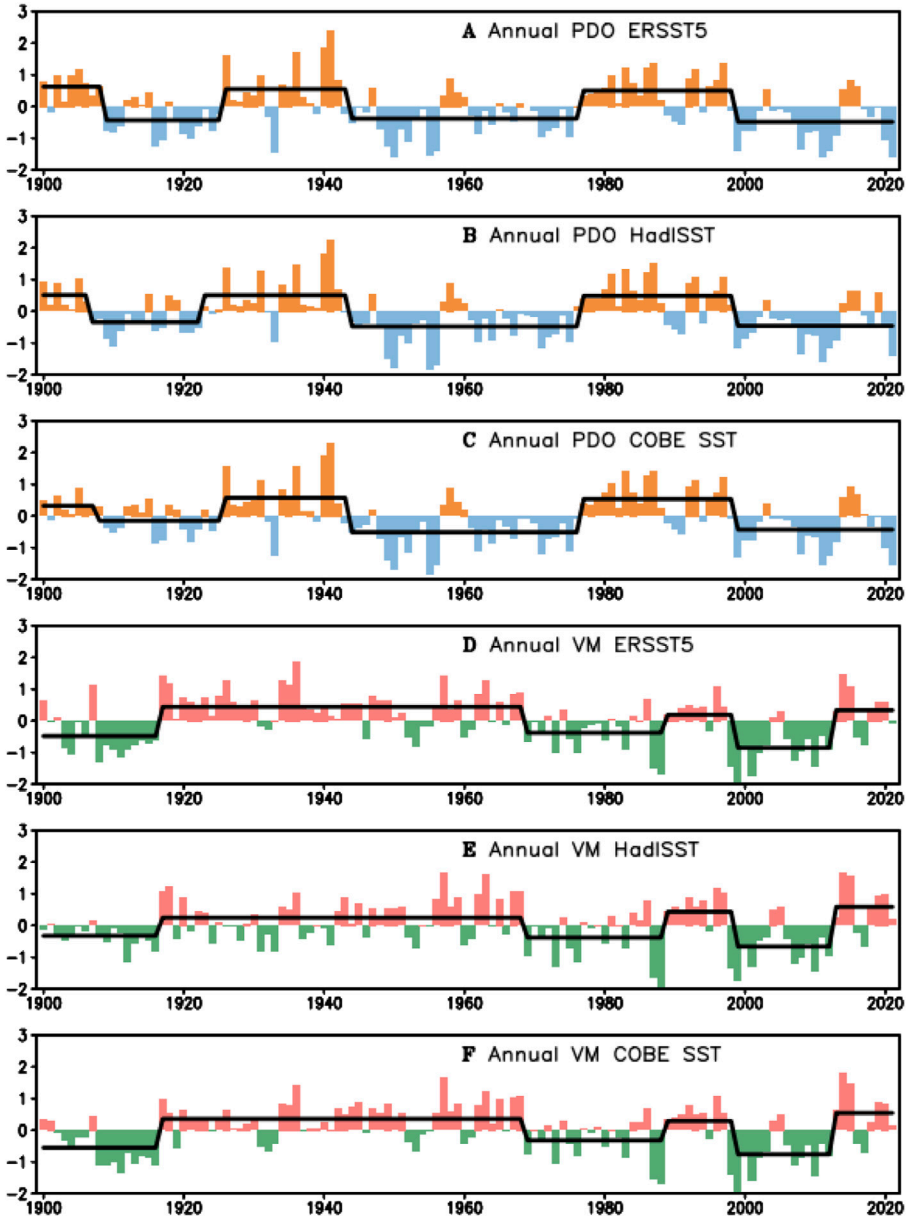

FIGURE 3
Similar to Figure 2, but for the annual mean PDO in **(A)** ERSST5, **(B)** HadISST, and **(C)** COBE SST, and annual mean VM in **(D)** ERSST5, **(E)** HadISST, and **(F)** COBE SST during 1900–2021.

(2013) with an enhancement of epoch mean of 0.33°C (0.61°C), and a decreased DAC in 1998 with a decrease of epoch mean of 0.20°C. The SST in Box 3 of HadISST experienced increased DACs in 1956, 1985, and 2013 with increases of mean values of 0.34°C, 0.40°C, and 0.50°C, and decreased DACs in 1969 and 1998 with decreases of the mean values of 0.26°C and 0.23°C, respectively (Figure 2J). In the COBE SST (Kaplan SSTA), there were increased DACs in 1956, 1985, and 2013 with increases of epoch average of 0.35 °C (0.39 °C), 0.20 °C (0.26 °C) and 0.49 °C (0.47 °C), and a decreased DAC in 1969 with a decrease of epoch mean of 0.22°C, respectively (Figures 2K, L). According to the time series of SST in the three boxes, it can be seen that there is a substantial sudden regime shift in 2013/14 in the North Pacific SST in above all SST data sets. The epoch means of SST in the above regions during 2014–2021 are at least the highest ones since the 1950s.

Generally, a mean state of a meteorological variable, which duration is equal (close) to or larger than 10 years, could be

considered as a decadal background (or mean state) itself. By the end of 2021, the mean state of SST during 2014–2021 has been maintained for 8 years already, which is less than 10 years. It is necessary to discuss whether the mean state during 2014–2021 can be distinguished from the previous mean state of SST in the North Pacific. In other words, did a regime shift occur in 2013/14? There are three reasons that we have the confidence to conclude that a new decadal regime shift happened in 2013/14, and a new decadal climate background is in place since 2014. Firstly, the mean value of the SST over the North Pacific has been sustained for 8 years which can be seen as a quasi-decadal regime shift so far. Furthermore, although the North Pacific SST in 2021 is relatively lower than the epochal mean of 2014–2021 due to the double La Niña, the mean value of 2014–2021 is significantly higher than the previous epoch mean of 1999–2013 (all exceeding the 99.9% confidence level). Even if the values of SST in 2022 and 2023 are equal to climate averaged value during 1950–2021, the mean value during 2014–2023 would be still significantly higher than that during 1998–2013. Secondly, we employed the moving *t*-test technique to examine the regime shift in 1997/98 in the study of Xiao and Li (2007a) by using the SST during 1854–2005. In this study, the epoch mean of SST in the central North Pacific during 1998–2005 also had maintained 8 years then. Now, the mean state after the regime shift 1997/98 had maintained at least 16 years by 2013 in the eastern North Pacific SST (Figures 2E–G) and 23 years by 2021 in the PDO index (Figures 3A–C). That is, the duration of the mean state (1998–2013 or 1998–2014) after the regime shift in 1997/98 is longer than the period of 1998–2005 when it was first found in the study (Xiao and Li, 2007a). The regime shift in 1997/98 has been widely accepted in climate research and it has been associated with important impacts on the global climate system (Hong et al., 2014; Doi et al., 2015; Dong and Dai, 2015; Jo et al., 2015; Zhu et al., 2015; Ellis and Marston, 2020; You et al., 2021). Thirdly, four SST data sets showed robust regime shift of North Pacific SST in 2013/14 not only in temporal evolution but also the spatial distribution. Based on the above reasons, the regime shift of the North Pacific SST in 2013/14 is very likely to be a true one.

The PDO and VM are defined as the leading and second EOF modes of the North Pacific SSTA north of 20°N, respectively. The Kaplan SSTA is an anomaly data set of SST. However, the climatological mean used for calculating the Kaplan SSTA data set is different from that in the EOF analysis used for calculating the PDO and VM indexes. Therefore, the PDO and VM indexes calculated by Kaplan SSTA cannot be used for comparision with those calculated by using the SST of ERSST5, HadISST, and COBE SST. Therefore, in this study, we showed the annual mean PDO and VM indexes in ERSST5, HadISST, and COBE SST data sets (Figure 3). The annual mean PDO indexes of ERSST5 (HadISST, COBE SST) experienced decreased DACs in 1909 (1907, 1907), 1943, and 1998, and the increased DACs in 1925 (1922, 1925) and 1976, respectively (Figures 3A–C). Although the horizontal distribution of the DACs is similar to the hoof pattern of the positive phase of the PDO mode, there is no regime shift in 2013/14 of the PDO index in the annual mean field in all these SST data sets. Furthermore, we also checked the November-March averaged PDO index, which displays the most distinguished decadal variability in these months (Mantua et al., 1997), and found no regime shift in the early-2010s (not shown).

The VM indexes in the data sets of ERSST5, HadISST, and COBE SST all experienced the DACs in 1916, 1968, 1988, 1998, and 2012, respectively (Figures 3D–F). The epoch means of the VM index increased 0.92 (0.56 and 0.91) after 1916, 0.57 (0.81 and 0.61) after 1988, and 1.19 (1.25 and 1.30) after 2012, and decreased 0.82 (0.62 and 0.68) after 1968 and 1.05 (1.09 and 1.05) after 1998 in ERSST5 (HadISST and COBE SST). These facts imply that the data sets of ERSST5, HadISST and COBE SST consistently reproduced the VM regime shifts, as well as their changes of epoch means. Compared with the regime shifts of PDO and VM, they did not occur at the same time except for that in 1998.

There seems to be a strange question about the regime shift in 2013/14. Although the horizontal distribution of the DACs in around 2013 presents a horseshoe pattern (Figures 1A–D), which resembles the SST anomalies along the western coast of North America in PDO mode, there is no (a) regime shift in 2013/14 in the PDO (VM) indexes in the three SST data sets. As shown in Figure 1 of the study by Ding et al. (2015b), the PDO mode shows negative anomalies over the region (125°E–140°W, 20°–50°N) and positive anomalies along the west coast of North America. The spatial pattern of the VM positive phase displays negative anomalies in the domain (125°E–160°W, 20°–35°N) and positive anomalies in other North Pacific regions. Compared to the horizontal distribution of the DACYs of SST in Figures 1A–D or the epoch mean SST difference between 2014–2021 and 1998–2013 (Figures 4E–H) with the PDO spatial mode, it can be found that there is no decreased DACs occurring in early-2010s (Figures 1A–D) and no obvious negative anomalies in epoch mean difference over the central North Pacific (Figures 4E–H). There are no decreased DACs of SST over the central North Pacific in the early-2010s. It is why the PDO did not experience a regime shift in 2013/14. With regard to the spatial pattern of VM, the region without significant anomalies in the central North Pacific (Figures 4E–H) corresponds well to the negative anomalous SST region in the positive phase of the VM pattern in Figure 1 from Ding et al. (2015b). The SST anomalies in other regions are all positive (Figures 4E–H), which also matches well the positive regions in the positive phase of the VM pattern in Figure 1 provided by Ding et al. (2015b). Therefore, from the pattern of SST difference of epoch mean before and after 2013, it also can be concluded that the VM (PDO) index experienced (doesn't experience) a regime shift in 2013/14.

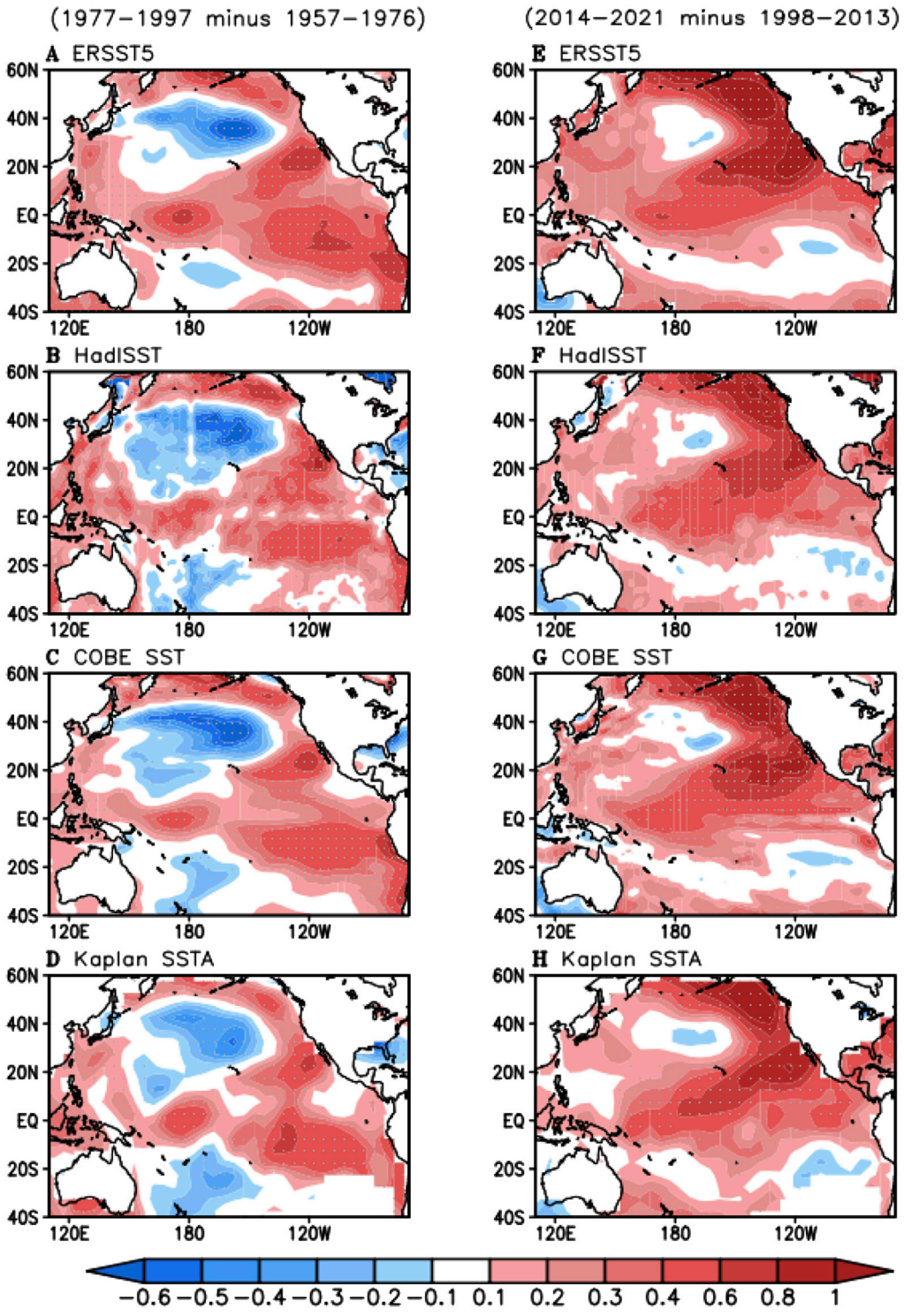

FIGURE 4
Composite differences (shading) of annual mean SST **(A)** between 1977–1997 and 1957–1976 and between 2014–2021 and 1998–2013 in **(A,E)** ERSST5, **(B,F)** HadISST, **(C,G)** COBE SST, and **(D,H)** Kaplan SSTA. The unit is K (°C). The stippling in all the panels indicates a 95% confidence level.

A warming regime shift also occurred along the coast of North America and in 1976/77, to the north of central North Pacific in 1988/89 (Yeh et al., 2011; Xiao et al., 2012; Jo et al., 2013; Song et al., 2020), and in the West Pacific and central North Pacific in 1997/98 (Xiao and Li, 2007a; Yeh et al., 2011; Jo et al., 2013; Hong et al., 2014; Doi et al., 2015; Jo et al., 2015; Song et al., 2020). The warming regime shift in the northern North Pacific in the late-1980s was associated with the meridional atmospheric mass exchange between the Arctic and mid-latitudes (Xiao et al., 2012). The regime shift occurring in the central North Pacific SST in 1997/98 refers to the phase reversal of the PDO and IPO and their wide impacts on the surrounding Pacific (Xiao and Li, 2007a; Yeh et al., 2011; Jo et al., 2013; Hong et al., 2014; Doi et al., 2015; Jo et al., 2015; Song et al., 2020).

The regime shift also happened in the North Pacific SST in 1976/77 which also displayed a warm hoof pattern along the western coast of North America (Xiao and Li, 2007b), similar to the pattern of the regime shift in 2013/14. It is interesting whether there are differences between these two regime shifts. Because there are also increased DACs in the North and South Pacific SST in 1956/57 and 1997/1998 (Xiao and Li 2007a), we employed the composite difference of SST between the period of 1977–1997 and 1957–1976 (2014–2021 and 1998–2013) to show the change in background state after the regime shift in 1976/77 (2013/14) in Figure 4. In Figure 4A, the composite difference of SST between 1977–1997 and 1957–1976 in ERSST5 displayed significant warming anomalies along the Pacific coast and over the Central Pacific with maximum anomalies of 0.6°C over the southeastern North Pacific, Bristol Gulf, central-east Pacific and significant cooling anomalies over the central North Pacific with the maximum value of −0.6°C and weaker cooling over the western South Pacific. The IPO is based here on the Triple index, which is calculated by subtracting the averaged North and South Pacific SSTA from those over the Tropical central-east Pacific SSTA (Henley et al., 2015). Therefore, the composite difference of SST is negative over the central North Pacific and eastern South Pacific and positive over the other Pacific region (Figure 4A), which suggests a positive phase of IPO and PDO. The phase transitions in the time series of PDO and IPO indexes also support their regime shifts in 1976/77 (Mantua et al., 1997; Henley et al., 2015). The SST difference in ERSST5 between 2014–2021 and 1998–2013 shows a remarkable warm horseshoe pattern over the North Pacific (Figure 4B) with SST anomalies up to 1°C. However, there are no obvious negative SST anomalies over the central North Pacific and South Pacific and no significant positive SST anomalies over the Equatorial East Pacific and eastern South Pacific. The positive-phase IPO mode shows warm anomalies over the Tropical East Pacific and negative anomalies over the North and South Pacific (Henley et al., 2015). Hence, the difference of SST over the Pacific between 2014–2021 and 1998–2013 suggests no regime shift of IPO and PDO happening in 2013/14. The time series of the IPO index indicates the regime shift in 1976/77 and no regime shift in 2013/14 (not shown). Therefore, the regime shift of Pacific SST in 1976/77 (2013/14) suggests either (neither) a phase transition of IPO or (nor) that of PDO.

The SST differences in HadISST (Figure 4B), COBE SST (Figure 4C), and Kaplan SSTA (Figure 4D) between 1977–1997 and 1957–1976 are generally similar to that in ERSST5. However, the domains of cold SST anomalies over the central North Pacific and eastern South Pacific are larger than that in ERSST5. Regarding the difference in SST between 2014–2021 and 1998–2013, the distributions of SST anomalies in HadISST (Figure 4B), COBE SST (Figure 4C), and Kaplan SSTA (Figure 4D) show high similarity to that in ERSST5. These facts support that the distribution of SST changes due to the regime shift in 1976/77 and 2013/14 are robust in the four SST data sets examined in this study.

Accompanied by the new regime shift in 2013/14, the global annual mean SAT and precipitation also changed significantly. The annual mean SAT over Alaska, the western and eastern United States, Europe, and northern Asia dramatically increased during 2014–2021 with the warming surpassing 2.0°C (Figure 5A). Such warmer temperatures in Siberia and western North America may be related to the warmer SST along North America. The warmer SST along North America can weaken the Siberia High and thereby induce warming over the northern Eurasian continent (Li et al., 2020) and induce weaker SLP anomalous over the North Pacific and warmer SAT over western North America (Deser et al., 2004). The well-known Warm-Arctic-Cold-Landmass pattern is a pattern with warm SAT anomalies over the Barents-Kara sea region and accompanied cold anomalies over Northeast Asia (Cohen et al., 2013). This pattern presented a positive phase during the hiatus or global warming slowdown period and a normal phase since 2014 (Trenberth, 2015). The above facts suggest the end of the Hiatus or global warming slowdown and the Warm-Arctic-Cold-Landmass pattern may be related to the regime shift of 2013/14, which is an interesting topic and needs further study. Under the global warming situation, there are, however, cooling anomalies over northeastern Canada and southwestern Greenland with significant anomalies of more than −1.5°C. Significant warming also appears over Australia and South America, but not as lager as these over northern Asia. The annual precipitation anomalies between 2014–2021 and 1998–2013 show more precipitation over East China, India, Central and East America, and East and West Africa and less precipitation over the Indochina Peninsula, Tropical South America, Australia, South Africa, and Europe. Generally, the annual mean precipitation increased (decreased) over most parts of the Northern (Southern) Hemispheric landmass monsoon regions. Wang et al. (2012) show the increasing trend of Northern Hemisphere monsoon (May-September) precipitation anomalies during 1979–2008, which is accompanied by warmer simulated SST in the Northern Hemisphere Ocean and warmer land SAT than the ocean and

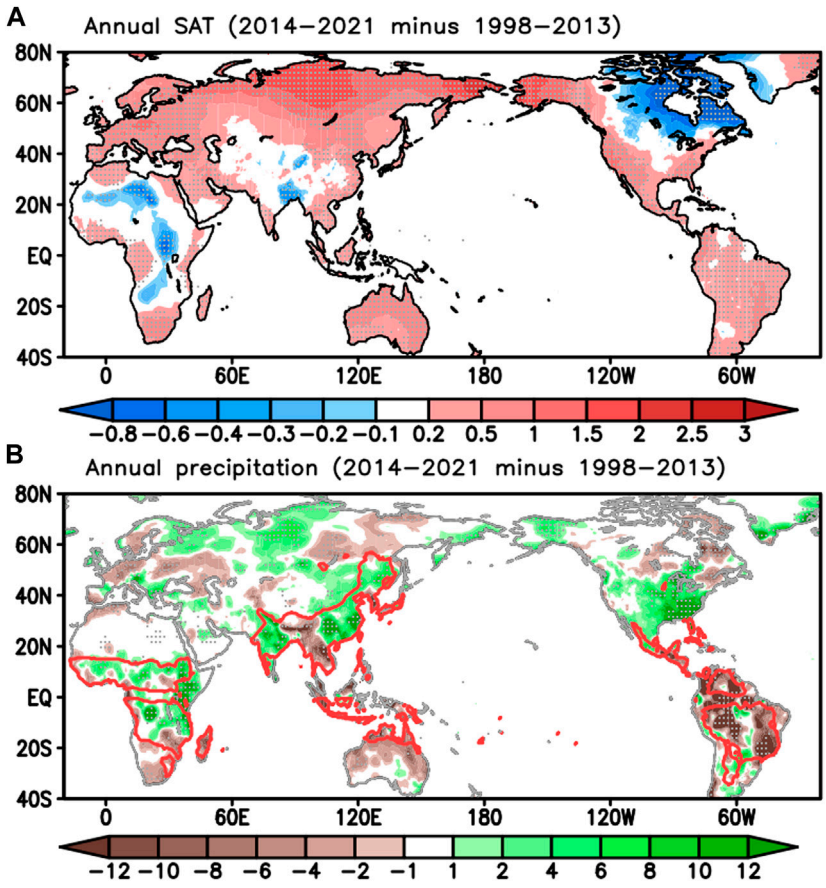

FIGURE 5
Composite differences (shading) of the annual mean **(A)** SAT and **(B)** precipitation from CRU between 2014–2021 and 1998–2013. The units are K (°C) and mm, respectively. The stippling in all the panels denotes the 95% confidence level. The red thickened line refers to the monsoon regions according to the definition by Wang and Ding (2006).

warmer SAT in the Northern Hemisphere than Southern Hemisphere. We speculate that the rainfall changes in the monsoon regions may be related to the SAT difference between land and ocean and between Northern and Southern Hemisphere. This is a very interesting topic which needs further studies.

Discussion

The mechanisms of decadal variability in the North Pacific SST have attracted wide attention over the past 3 decades. Generally, the origin of the decadal variability of the North Pacific has been attributed to the extratropics and to the remote tropics (Alexander et al., 1999; Alexander et al., 2002; Liu et al., 2002; Newman et al., 2003; Liu and Alexander, 2007; Liu, 2012; Liu, 2015; Newman et al., 2016; Liu and Di Lorenzo, 2018), as well as the Atlantic Ocean (Johnson et al., 2020). We examined the annual mean Atlantic Multi-decadal Oscillation (AMO) index (Enfield et al., 2001) and there is no regime shift occurring in the early-2010s (not shown). Therefore, here we reviewed the mechanisms of the North Pacific decadal variability from extratropics and the remote tropics and discussed the possible cause of the regime shift of the North Pacific SST in 2013/14.

Mid-latitude oceanic and atmospheric dynamics

The mechanisms over the extratropical ocean and atmosphere systems involved the Aleutian Low stochastic forcing and the mid-latitude ocean-atmosphere coupling. The stochastic noise forcing can generate a slow dynamical response (Hasselmann, 1976) and produce a reddening noise spectrum of SST anomalies (Frankignoul and Hasselmann, 1977), as well as in

the entire North Pacific basin (Frankignoul and Reynolds, 1983). The interannual variability of surface flux and SST anomalies are closely related to the dominant atmospheric patterns, namely the Aleutian Low, whose intensity can be indicated by the dominant SLP pattern and result from the internal atmospheric dynamics (Cayan, 1992). Simulated anomalous Ekman transports tend to enhance the flux-driven pattern, which is similar to the low-frequency pattern in the North Pacific (Miller et al., 1994; Alexander and Scott, 2008). Theory, model, and dynamical diagnosis suggest the stochastic noise in the mid-latitude is a key driving forcing for the Pacific decadal variability modes, including the PDO, IPO or Pacific multidecadal variability and North Pacific Gyre Oscillation (Liu 2015).

Another extratropical mechanism is the North Pacific coupled oceanic and atmospheric mechanism. Latif and Barnett (1994) simulated a quasi-20-year variability in North Pacific and proposed that the origin of the North Pacific decadal variability is in the extratropics. However, most of the above mechanism was later demonstrated to be invalid or questionable (Alexander et al., 1999; Deser et al., 1999; Schneider and Miller, 2001). Schneider et al. (2002) suggest that the Latif and Barnett mechanism represents an atmospheric-stochastically-driven oceanic mode, rather than a coupled ocean-atmosphere mode as described in the original hypothesis (Liu, 2012).

Tropical forcing *via* atmospheric teleconnection

The spatial pattern of SST associated with the low frequency (>6 years) resembles that of the low frequency of ENSO (Zhang et al., 1997). Tropical Pacific decadal variations can drive approximately 1/4–1/2 variability in North Pacific based on the general circulation model (Alexander et al., 2002). ENSO is the primary forcing for the North Pacific SST on interannual variability *via* atmospheric teleconnection and subsequent changes in Aleutian Low variability (Trenberth et al., 1998). Anomalous tropical convection induced by ENSO influences the global atmospheric circulation and alters surface fluxes over the North Pacific and deepens the Aleutian Low *via* a reduction in the climatological-mean zonal SST gradient, forcing SST anomalies that peak a few months after the ENSO maximum in the Equatorial East Pacific SST (Trenberth and Hurrell, 1994; Alexander et al., 2002; Gan et al., 2017).

Possible cause of the regime shift in 2013/14

According to the discussions, the Equatorial Central and East Pacific (EMEP) SST can influence the variation of the Aleutian Low, which further impact the North Pacific SST (Trenberth and Hurrell, 1994). Therefore, we examined the leading and lagged relationship among them by HadISST with high resolution in the equator during the periods of 1957–1997 and 1998–2021, which corresponds to the periods in Figure 4. The results are similar to those in the data sets of ERSST5, COBE SST, and Kaplan SSTA. The EMEP SST was averaged from the region 80°–170°W, 5°S–5°N. The North Pacific SST was averaged in the three boxes in Figure 1. The North Pacific Index (NPI), which represents the mean intensity of the Aleutian Low (Trenberth and Hurrell, 1994), was averaged from the monthly SLP over the North Pacific (160°E–140°W, 30°–65°N). During the period of 1957–1997, the EMEP SST was leading to the NPI 3 months (light blue solid line), and the NPI was leading to the North Pacific SST 2 months (light green solid line). These results imply a possible influencing relationship of EMEP SST–NPI–North Pacific SST. Such a relationship suggests a possible mechanism that the EMEP SST influences the Aleutian Low and further forces the North Pacific SST, which supports the tropical-oriented mechanism proposed by Trenberth and Hurrell (1994). Different from the period of 1957–1997, there is no leading or lagged correlation between EMEP SST and NPI during 1998–2021 (light blue dashed line). Such facts imply that the tropical influence on the North Pacific atmosphere does not work during this period. Therefore, it is inferred that the regime shift in 2013/14 in the North Pacific SST may not be influenced by EMEP SST and may originate from the extratropical region.

It is necessary to explain the difference between the leading and lagged relationship between EMEP and North Pacific SSTs and that inferred from the leading and lagged correlation among EMEP, NPI, and North Pacific SST. For example, the leading and lagged correlation during 1957–1997 showed that the EMEP SST (NPI) was leading the NPI (North Pacific SST) by 3 (2) months. We should not infer that the EMEP SST was leading the North Pacific SST by 5 months. In fact, the EMEP SST and North Pacific SST are simultaneously correlated and there is no leading and lagged correlation between them during 1957–1997 (Figure 6). The leading and lagged correlation during 1957–1997 shows a possible relationship of EMEP SST–NPI–North Pacific SST. The EMEP SST has no leading and lagged relationship with the North Pacific SST. Similarly, the possible relationship during 1998–2013 among them is NPI–North Pacific SST–EMEP SST. Such a relationship implies that the stochastic noise over the North Pacific may influence the variation of the North Pacific SST, which further acts on the EMEP SST. The beginning variable of this relationship (NPI) is simultaneously correlated with the last variable (EMEP SST). The two variables simultaneously correlated in the two relationships can be distinguished as the beginning and ending variables of the relationships, respectively. Therefore, the relationship between EMEP and North Pacific SSTs should be calculated by leading and lagged correlation instead of inferring from the leading and lagged correlations among EMEP, NPI, and North Pacific SST.

The EMEP SST, NPI, and North Pacific SST all experienced the regime shift in 1976/77 (Nitta and Yamada, 1989; Trenberth and Hurrell, 1994; Mantua et al., 1997; Power et al., 1999; Xiao and Li, 2007b). According to the leading and lagged correlation

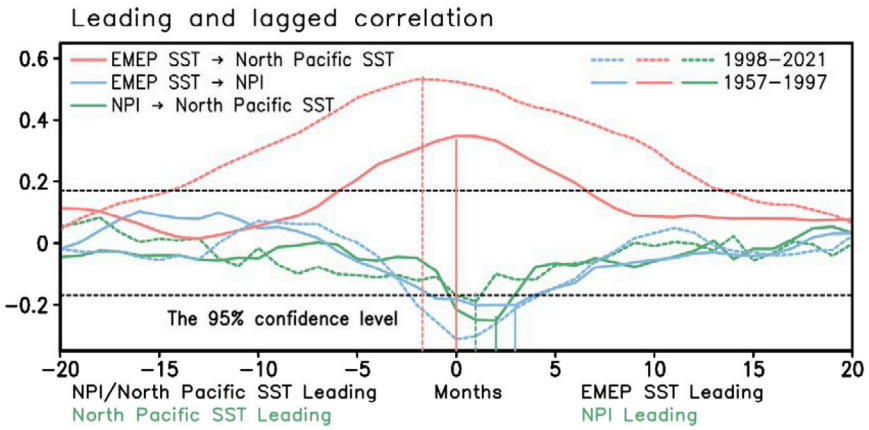

FIGURE 6
Leading and lagged correlation between EMEP SST (EMEP SST, NPI) and North Pacific SST (NPI, North Pacific SST) during 1957–1997 and 1998–2021, respectively. For example, the EMEP SST → North Pacific SST symbol denotes the correlation of the EMEP SST leading to the North Pacific SST. The horizontal dashed lines refer to the 95% confidence level based on the effective degrees of freedom. The solid and dashed colored curves denote the correlations during 1957–1997 and 1998–2021, respectively. The vertical colored solid and dashed lines show the positions of the maximal absolute value of the same colored curves.

during 1957–1997, the tropical influence mechanism on the regime shift of the North Pacific SST in 1976/77 by the Aleutian Low can be established and support that proposed by Trenberth and Hurrell (1994). During the period of 1998–2021, the NPI was 1 month leading to the North Pacific SST, which was 2 months leading to the EMEP SST, and the EMEP SST was only simultaneously correlated with the NPI (Figure 6). These facts suggest the influence of NPI on EMEP SST by modulating the North Pacific SST on a monthly time scale during 1998–2021. Furthermore, it is interesting whether there is a possible mechanism of the influence of Aleutian Low on EMEP SST by modulation on the North Pacific SST during 1998–2021 on a decadal time scale. The EMEP SST does not show a regime shift in 2013/14 (Figure 1). Hence, the regime shift of North Pacific SST in 2013/14 cannot be attributed to the tropical influence mechanism and cannot result in the regime shift of EMEP SST. The NPI is still leading the North Pacific SST by 1 month during the period of 1998–2021. It is still unclear whether the regime shift of North Pacific SST in 2013/14 is attributed to that of the North Pacific atmosphere. Therefore, we show the central intensity of Aleutian Low and the annual NPI index (Figure 7). Following the study of Overland et al. (1999), the central intensity of Aleutian Low is defined as January-February (JF) averaged minimal SLP in the North Pacific region (160°E–140°W, 40°–65°N). It witnessed the regime shift in 1988/89, 1996/97, and 2005/06 (Figure 7A). The regime shifts of the annual mean NPI happened in 2005/06. There is no regime shift in 2013/14 in both JF central intensity and annually averaged intensity of the Aleutian Low. These facts imply that the regime shift of the North Pacific SST in 2013/14 may not be a result of the midlatitude atmospheric forcing on decadal time scale. Namely, the Aleutian Low driven EMEP SST variation by the influence on North Pacific SST may work on a high-frequency (monthly) time scale instead of a decadal time scale.

Figure 7B shows the JF central locations of the Aleutian Low during the periods of 1989–1996, 1997–2005, and 2006–2022. These three periods are divided by the regime shift in JF central intensity of the Aleutian Low (Figure 7A). The JF central locations of the Aleutian Low during 1979–1988 are not shown because of their similarity to those in 1997–2005. Half of the centers of Aleutian Low during 1989–1996 were located to the west of the dateline (Figure 7B). The centers of JF Aleutian Low in 1992 and 1995 were located along the longitude 180° and 160°W, which may be related to the warm surface condition over the North Pacific Ocean induced by the El Niño in 1991/92 and 1994/95. The locations of the Aleutian Low centers during 1997–2005 were all to the east of the dateline. That is, the central locations of Aleutian Low shifted eastward after the regime shift in 1996/97, which may be related to the warming regime shift of the central North Pacific at the same time. There were 13 centers of the Aleutian Low during 2006–2022 located to the west of the dateline (including the year 2007, when the location was very close to the dateline) and 5 centers approximately along the longitude 150°–160°W. The center locations of JF Aleutian Low in the years 2010, 2015, and 2016 were also corresponding to the El Niño in 2009/10, 2014/15, and 2015/16. These facts suggest that the central locations of the Aleutian Low shift back to the west of the dateline after the regime shift in 2005/06. Except for the years 2014–2016, there were 6 years (2017–2022) of JF Aleutian Low centers located to the west of the dateline. That is, there is no regime shift in 2013/14 of the central location of JF Aleutian Low. Therefore, there is no regime shift occurring in 2013/14 in JF central intensity and central locations and the annual mean intensity of Aleutian Low. Therefore, we may not attribute the

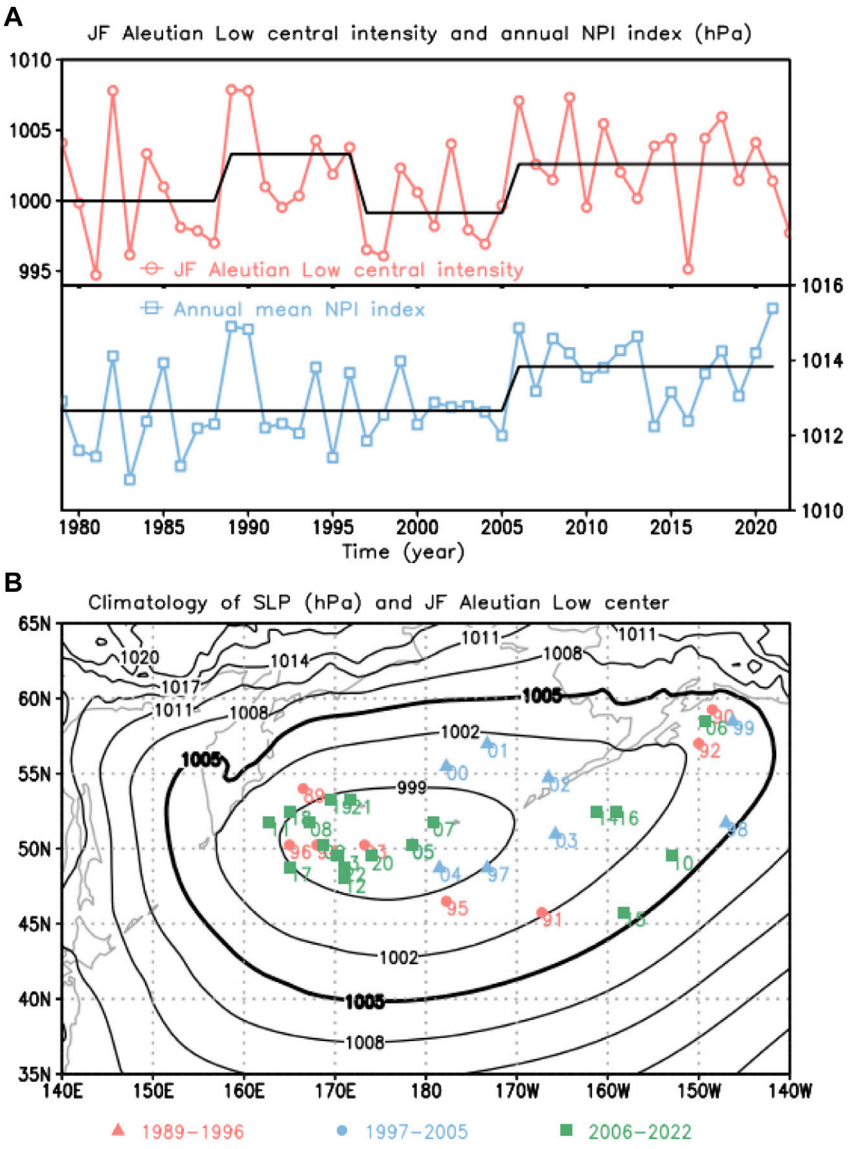

FIGURE 7
(A) JF Aleutian Low central intensity (light red line with circle) and annual mean NPI (light blue with square) and their epoch average (thicken solid line) divided by the DACYs examined by the moving *t*-test technique at the 95% confidence level. **(B)** Climatology (contour) of JF SLP and JF Aleutian Low central locations in three periods of 1989–1996 (light red solid triangle), 1997–2005 (line blue solid dot), and 2006–2022 (light green solid box). The years of the Aleutian Low central locations are drawn on the right of the marks. The interval of the contour is 3 and the unit is hPa. The contour of 1005 hPa is thickened to indicate the climatological Aleutian Low domain.

regime shift of North Pacific SST in 2013/14 to a response to the decadal variation of North Pacific atmospheric forcing.

According to the occurring time, the regime shift in 1988/89 of JF central intensity of the Aleutian Low (Figure 7A) may be related to the regime shift of the VM index in 1988/89 (Figures 3D–F). Similarly, the regime shift in 1996/97 (Figure 7A) maybe has a relationship with the regime shift of PDO in 1997/98 (Figures 3A–C). The regime shift in 2005/06 of both the JF central intensity and annual mean intensity of the Aleutian Low (Figure 7A) may be related to the regime shift of the Kara-Barent Sea ice concentration, which also experienced a regime shift in 2005/06 (Xiao et al., 2021). The connection between the intensity and locations of the Aleutian Low with these regime shifts needs further studies.

Summary and conclusion

We found a new regime shift of SST over the North Pacific in 2013/14, showing a horseshoe shape with a band of significantly warmer SST along the west coast of North America and over the

northern Tropical Central Pacific, robust among the data sets of ERSST5, HadISST, COBE SST, and Kaplan SSTA. The time series of the SST over the horseshoe region show a significant regime shift in 2013/14 in all the above SST datasets, with a significant increase of SST epoch mean up to 0.97 C. The mean values of SST in the above regions during 2014–2021 are much larger than those in previous epochs since 1950. Although the distribution of the DACYs, showing a hoof pattern along the western coast of North America, resembles a PDO mode, the PDO index does not experience a regime shift in 2013/14, due to no decreased DACs of SST or even increased DACs of SST occurring in the central North Pacific. On the other hand, the VM index witnessed the regime shift in 2013/14 because the domain with insignificant anomalies in the North Pacific well matched the negative anomalous region in the VM positive phase.

The composite difference of SST over the North Pacific between 2014–2021 and 1998–2012 showed a similar pattern to that between 1977–1997 and 1957–1976. However, there were no significant positive SST anomalies over the Tropical East Pacific and negative SST anomalies over the North and South Pacific, implying no regime shift of IPO and PDO in 2013/14. Therefore, the regime shift in 1976/77 (2013/14) suggests that there are (no) phase transitions of IPO and PDO on a decadal time scale.

The annual mean SAT over the high-latitude continent in the Northern and Southern Hemispheres during 2014–2021 is significantly larger than in the previous period of 1998–2013. The difference in SST between 2014–2021 and 1998–2013 displays up to 2°C warming over the northern Eurasia landmass, Alaska, and western North America. Nevertheless, there are also significant negative anomalies over Northeast Canada and southwestern Greenland, with a maximal value of −1.5°C. The precipitation during 2014–2021 generally increased in the northern hemispheric regions of East Asian monsoon, Indian monsoon, West African monsoon, and North American monsoon and decreased over the Australian and South American monsoon regions.

The EMEP SST (NPI) was leading the NPI (North Pacific SST) 3 (2) months during 1957–1997. It can be inferred the modulation of the tropical Pacific Ocean on the North Pacific SST by the midlatitude atmospheric forcing, which supports the mechanism proposed by Trenberth and Hurrell (1994). The leading and lagged relation during 1998–2021 showed that the NPI (North Pacific SST) is 1 (2) month(s) leading to the North Pacific (EMEP) SST. It suggests an influencing relationship between NPI-North Pacific SST-EMEP SST during 1998–2021. The EMEP SST does not experience the regime shift approximated in 2013/14, as well as the central intensity and locations and annual mean intensity of Aleutian Low. These findings suggest that the origin of the regime shift in 2013/14 of North Pacific SST may be not the decadal variation of the North Pacific atmosphere and EMEP SST, and may be related to the high-frequency midlatitude atmospheric forcing.

The PDO plays an important role in the modulation of the warming pace of the global SAT (Trenberth, 2015; Iselin Medhaug et al., 2017). The negative phase of PDO can effectively slow down the pace of global warming (Mochizukia et al., 2010) by decreasing the Siberian SAT (Li et al., 2020). During the period of 1943–1976, a positive phase of the PDO, the global temperature experienced a fast warming period. During the period from 1998 to 2013, global warming witnessed a slowdown or hiatus. The hiatus faded away since the year 2014 (Zhang et al., 2019). That is, the ending of the hiatus is roughly corresponding to the regime shift over the North Pacific in 2013/14. However, the PDO did not experience (VM experienced) a regime shift in 2013/14. There are, as a result, interesting questions as follows: Is the decadal phase transition of PDO still anchored to the beginning and end of the global warming slowdown? Or does the cessation of the global warming slowdown start to anchor the phase transition of the VM index? There is no regime shift in 2013/14 happening in central North Pacific SST. Is the spatial pattern of PDO under the global warming background different from the previous one? Plenty of the influences on many aspects of the atmospheric, oceanic and ecological system of this regime shift are still open questions. These questions are very interesting and warrant further investigations.

Data availability statement

The original contributions presented in the study are included in the article/supplementary material, further inquiries can be directed to the corresponding author.

Author contributions

DX contributed to designing the study, performing analyses, and writing the paper. H-LR assisted with the framing and development of ideas and reviewed the manuscript.

Funding

This work was jointly supported by the Second Tibetan Plateau Scientific Expedition and Research (STEP) program (2019QZKK0105) and the Strategic Priority Research Program of the Chinese Academy of Sciences (XDA20100300), National Science Foundation of China grant (42175053 and 41775066) and Natural Science Foundation of Shanghai (21ZR1457600).

Acknowledgments

The authors thank the Met Office Hadley Centre, National Ocean and Atmosphere Administration (NOAA) Physical Sciences Laboratory (PSL) for offering the SST data sets and many climate indexes, and also thank Climate Research Unit for offering the

monthly global landmass SAT and precipitation. We also appreciate Ding Rui-Qing for offering the VM index.

Conflict of interest

The authors declare that the research was conducted in the absence of any commercial or financial relationships that could be construed as a potential conflict of interest.

Publisher's note

References

Alexander, M. A., Deser, C., and Timlin, M. (1999). The reemergence of SST anomalies in the North Pacific ocean. *J. Clim.* 12, 2419–2433. doi:10.1175/1520-0442(1999)012<2419:trosai>2.0.co;2

Alexander, M., Blade, I., Newman, M., Lanzante, J. R., Lau, N. C., and Scott, J. D. (2002). The atmospheric bridge: The influence of ENSO teleconnections on air-sea interaction over the global oceans. *J. Clim.* 15, 2205–2231. doi:10.1175/1520-0442(2002)015<2205:tabtio>2.0.co;2

Alexander, M. A., Matrosova, L., Penland, C., Scott, J. D., and Chang, P. (2008). Forecasting pacific SSTs: Linear inverse model predictions of the PDO. *J. Clim.* 21, 385–402. doi:10.1175/2007jcli1849.1

Alexander, M. A., and Scott, J. D. (2008). The role of Ekman ocean heat transport in the Northern Hemisphere response to ENSO. *J. Clim.* 21, 5688–5707. doi:10.1175/2008jcli2382.1

Bond, N. A., Overland, J. E., Spillane, M., and Stabeno, P. (2003). Recent shifts in the state of the North Pacific. *Geophys. Res. Lett.* 30, 2183. doi:10.1029/2003gl018597

Cayan, D. R., Dettinger, M. D., Diaz, H. F., and Graham, N. E. (1998). Decadal variability of precipitation over Western North America. *J. Clim.* 11, 3148–3166. doi:10.1175/1520-0442(1998)011<3148:dvopow>2.0.co;2

Cayan, D. R. (1992). Latent and sensible heat flux anomalies over the northern oceans: The connection to monthly atmospheric circulation. *J. Clim.* 5, 354–369. doi:10.1175/1520-0442(1992)005<0354:lashfa>2.0.co;2

Chavez, F., Ryan, J., Lluch-Cota, S., and iquen, M. (2003). From anchovies to sardines and back: Multidecadal change in the Pacific ocean. *Science* 299, 217–221. doi:10.1126/science.1075880

Cohen, J., Jones, J., Furtado, J., and Tziperman, E. (2013). Warm arctic, cold continents: A common pattern related to arctic sea ice melt, snow advance, and extreme winter weather. *oceanog.* 26, 150–160. doi:10.5670/oceanog.2013.70

Deser, C., Alexander, M. A., and Timlin, M. (1999). Evidence for a wind-driven intensification of the kuroshio current extension from the 1970s to the 1980s. *J. Clim.* 12, 1697–1706. doi:10.1175/1520-0442(1999)012<1697:efawdi>2.0.co;2

Deser, C., Phillips, A. S., and Hurrell, J. W. (2004). Pacific interdecadal climate variability: Linkages between the tropics and the North Pacific during boreal winter since 1900. *J. Clim.* 17, 3109–3124. doi:10.1175/1520-0442(2004)017<3109:picvlb>2.0.co;2

Ding, R., Li, J., Tseng, Y.-H., and Ruan, C. (2015a). Influence of the North Pacific Victoria mode on the pacific ITCZ summer precipitation. *J. Geophys. Res. Atmos.* 120, 964–979. doi:10.1002/2014jd022364

Ding, R., Li, J., Tseng, Y.-H., Sun, C., and Guo, Y. (2015b). The Victoria mode in the North Pacific linking extratropical sea level pressure variations to ENSO. *J. Geophys. Res. Atmos.* 120, 27–45. doi:10.1002/2014JD022221

Doi, T., Behera, S. K., and Yamagata, T. (2015). An interdecadal regime shift in rainfall predictability related to the Ningaloo Nino in the late 1990s. *J. Geophys. Res. Oceans* 120, 1388–1396. doi:10.1002/2014jc010562

Dong, B., and Dai, A. (2015). The influence of the interdecadal Pacific oscillation on temperature and precipitation over the globe. *Clim. Dyn.* 45, 2667–2681. doi:10.1007/s00382-015-2500-x

Easterling, D. R., and Peterson, T. C. (1995). A new method for detecting undocumented discontinuities in climatological time series. *Int. J. Climatol.* 15, 369–377. doi:10.1002/joc.3370150403

Ellis, A. W., and Marston, M. L. (2020). Late 1990s' cool season climate shift in eastern North America. *Clim. Change* 162, 1385–1398. doi:10.1007/s10584-020-02798-z

Enfield, D. B., Mestas-Nunez, A. M., and Trimble, P. J. (2001). The Atlantic Multidecadal Oscillation and its relation to rainfall and river flows in the continental U.S. *Geophys. Res. Lett.* 28, 2077–2080. doi:10.1029/2000gl012745

Francis, R., and Hare, S. (1994). Decadal-scale regime shifts in the large marine ecosystems of the North-east Pacific: A case for historical science. *Fish. Oceanogr.* 3, 279–291. doi:10.1111/j.1365-2419.1994.tb00105.x

Frankignoul, C., and Hasselmann, K. (1977). Stochastic climate models. Part II: Application to sea-surface temperature anomalies and thermocline variability. *Tellus* 29, 289–305. doi:10.1111/j.2153-3490.1977.tb00740.x

Frankignoul, C., and Reynolds, R. W. (1983). Testing a dynamical model for mid-latitude sea surface temperature anomalies. *J. Phys. Oceanogr.* 13, 1131–1145. doi:10.1175/1520-0485(1983)013<1131:tadmfm>2.0.co;2

Fu, C. B., and Wang, Q. (1992). The definition and detection of the abrupt climate change (in Chinese with English figure captions). *Chin. J. Atmos. Sci.* 16, 482–493. doi:10.3878/j.issn.1006-9895.1992.04.11

Gan, B., Wu, L., Jia, F., Li, S., Cai, W., Nakamura, H., et al. (2017). On the response of the aleutian low to greenhouse warming. *J. Clim.* 30, 3907–3925. doi:10.1175/jcli-d-15-0789.1

Han, W., Meehl, G. A., Hu, A., Alexander, M. A., Yamagata, T., Yuan, D., et al. (2014). Intensification of decadal and multi-decadal sea level variability in the Western tropical Pacific during recent decades. *Clim. Dyn.* 43, 1357–1379. doi:10.1007/s00382-013-1951-1

Hare, S. R., and Mantua, N. J. (2000). Empirical evidence for North Pacific regime shifts in 1977 and 1989. *Prog. Oceanogr.* 47, 103–145. doi:10.1016/s0079-6611(00)00033-1

Harris, I., Osborn, T. J., Jones, P., and Lister, D. (2020). Version 4 of the CRU TS monthly high-resolution gridded multivariate climate dataset. *Sci. Data* 7, 109. doi:10.1038/s41597-020-0453-3

Hasselmann, K. (1976). Stochastic climate models. Part I. Theory. *Tellus* 28, 473–485. doi:10.1111/j.2153-3490.1976.tb00696.x

He, W., Feng, G., Wu, Q., He, T., Wan, S., and Chou, J. (2012). A new method for abrupt dynamic change detection of correlated time series. *Int. J. Climatol.* 32, 1604–1614. doi:10.1002/joc.2367

He, W., Wan, S., Jiang, Y., Zhang, W., Wu, Q., and He, T. (2013). Detecting abrupt change on the basis of skewness: Numerical tests and applications. *Int. J. Climatol.* 33, 2713–2727. doi:10.1002/joc.3624

He, W., Liu, Q., Jiang, Y., and Lu, Y. (2015). Comparison of performance between rescaled range analysis and rescaled variance analysis in detecting abrupt dynamic change. *Chin. Phys. B* 24, 049205. doi:10.1088/1674-1056/24/4/049205

He, W., Liu, Q., Gu, B., and Zhao, S. (2016). A novel method for detecting abrupt dynamic change based on the changing Hurst exponent of spatial images. *Clim. Dyn.* 47, 2561–2571. doi:10.1007/s00382-016-2983-0

Henley, B. J., Gergis, J., Karoly, D. J., Power, S. B., Kennedy, J., and Folland, C. K. (2015). A tripole index for the interdecadal pacific oscillation. *Clim. Dyn.* 45, 3077–3090. doi:10.1007/s00382-015-2525-1

Hersbach, H., Bell, B., Berrisford, P., Hirahara, S., Horányi, A., Muñoz-Sabater, J., et al. (2020). The ERA5 global reanalysis. *Q. J. R. Meteorol. Soc.* 146, 1999–2049. doi:10.1002/qj.3803

Hong, C.-C., Wu, Y.-K., Li, T., and Chang, C.-C. (2014). The climate regime shift over the Pacific during 1996/1997. *Clim. Dyn.* 43, 435–446. doi:10.1007/s00382-013-1867-9

Hu, Z., and Huang, B. (2009). Interferential impact of ENSO and PDO on dry and wet conditions in the US great plains. *J. Clim.* 22, 6047–6065. doi:10.1175/2009jcli2798.1

Huang, B., Thorne, P., Banzon, V. F., Boyer, T., Chepurin, G., Lawrimore, J., et al. (2017). Extended reconstructed Sea Surface temperature, version 5 (ERSSTv5): Upgrades, validations, and intercomparisons. *J. Clim.* 30, 8179–8205. doi:10.1175/jcli-d-16-0836.1

Iselin medhaug, B., Stolpe, M., Fischer, E., and Knutti, R. (2017). Reconciling controversies about the 'global warming hiatus. *Nature* 545, 41–47. doi:10.1038/nature22315

Ishii, M., Shouji, A., Sugimoto, S., and Matsumoto, T. (2005). Objective analyses of sea-surface temperature and marine meteorological variables for the 20th century using ICOADS and the kobe collection. *Int. J. Climatol.* 25, 865–879. doi:10.1002/joc.1169

Jin, H. M., He, W. P., Liu, Q. Q., Wang, J. S., and Feng, G. L. (2016). The applicability of research on moving cut data-approximate entropy on abrupt climate change detection. *Theor. Appl. Climatol.* 124, 475–486. doi:10.1007/s00704-015-1428-8

Jo, H.-S., Yeh, S.-W., and Kim, C.-H. (2013). A possible mechanism for the North Pacific regime shift in winter of 1998/1999. *Geophys. Res. Lett.* 40, 4380–4385. doi:10.1002/grl.50798

Jo, H.-S., Yeh, S.-W., and Lee, S.-K. (2015). Changes in the relationship in the SST variability between the tropical Pacific and the North Pacific across the 1998/1999 regime shift. *Geophys. Res. Lett.* 42, 7171–7178. doi:10.1002/2015gl065049

Johnson, Z. F., Chikamoto, Y., Wang, S., Mcphaden, M. J., and Mochizuki, T. (2020). Pacific decadal oscillation remotely forced by the equatorial Pacific and the Atlantic oceans. *Clim. Dyn.* 55, 789–811. doi:10.1007/s00382-020-05295-2

Kaplan, A., Cane, M., Kushnir, Y., Clement, A., Blumenthal, M., and Rajagopalan, B. (1998). Analyses of global sea surface temperature 1856-1991. *Deleted DOIs* 103, 18567–18590. doi:10.1029/98jc01736

Krishnan, R., and Sugi, M. (2003). Pacific decadal oscillation and variability of the Indian summer monsoon rainfall. *Clim. Dyn.* 21, 233–242. doi:10.1007/s00382-003-0330-8

Latif, M., and Barnett, T. P. (1994). Causes of decadal climate variability over the North Pacific and NorthNorth America. *Science* 266, 634–637. doi:10.1126/science.266.5185.634

Lee, S. H., Seo, K. H., and Kwon, M. (2019). Combined effects of El Niño and the Pacific decadal oscillation on summertime circulation over East Asia. *Asia-Pacific J. Atmos. Sci.* 55, 91–99. doi:10.1007/s13143-018-00103-8

Li, G., Chen, J., Wang, X., Tan, Y., and Jiang, X. (2017). Modulation of Pacific Decadal Oscillation on the relationship of El Niño with southern China rainfall during early boreal winter. *Atmos. Sci. Lett.* 18, 336–341. doi:10.1002/asl.761

Li, B., Peng, L., Yaning, C., Zhang, B., and Shi, X. (2020). Recent fall Eurasian cooling linked to North Pacific sea surface temperatures and a strengthening Siberian high. *Nat. Commun.* 11, 5202. doi:10.1038/s41467-020-19014-2

Liu, Z., Wu, L., Gallimore, R., and Jacob, R. (2002). Search for the origins of Pacific decadal climate variability. *Geophys. Res. Lett.* 29, 42-1–42-4. doi:10.1029/2001GL013735

Liu, Q., He, W., Gu, B., and Jiang, Y. (2017). Detecting abrupt dynamic change based on changes in the fractal properties of spatial images. *Theor. Appl. Climatol.* 130, 435–442. doi:10.1007/s00704-016-1889-4

Liu, Z., and Alexander, M. (2007). Atmospheric bridge, oceanic tunnel, and global climatic teleconnections. *Rev. Geophys.* 45, RG2005. doi:10.1029/2005rg000172

Liu, Z., and Di Lorenzo, E. (2018). Mechanisms and predictability of pacific decadal variability. *Curr. Clim. Change Rep.* 4, 128–144. doi:10.1007/s40641-018-0090-5

Liu, Z. (2012). Dynamics of interdecadal climate variability: A historical perspective. *J. Clim.* 25, 1963–1995. doi:10.1175/2011jcli3980.1

Liu, Z. (2015). "Chapter 10: A review of the dynamics of pacific interdecadal climate variability," in *World scientific series on asia-pacific weather and climate climate change: Multidecadal and beyond*. Editors C.-P. Chang, M. Ghil, M. Latif, and J. M. Wallace (World Scientific Press), 159–169.

Mantua, N. J., and Hare, S. R. (2002). The Pacific decadal oscillation. *J. Oceanogr.* 58, 35–44. doi:10.1023/a:1015820616384

Mantua, N. J., Hare, S. R., Zhang, Y., Wallace, J. M., and Francis, R. C. (1997). A Pacific interdecadal climate oscillation with impacts on salmon production. *Bull. Amer. Meteor. Soc.* 78, 1069–1079. doi:10.1175/1520-0477(1997)078<1069:apicow>2.0.co;2

Miller, A. J., Cayan, D. R., Barnett, T. P., Graham, N. E., and Oberhuber, J. M. (1994). Interdecadal variability of the Pacific ocean: Model response to observed heat flux and wind stress anomalies. *Clim. Dyn.* 9, 287–302. doi:10.1007/BF00204744

Minobe, S. (1997). A 50-70 year climatic oscillation over the North Pacific and NorthNorth America. *Geophys. Res. Lett.* 24, 683–686. doi:10.1029/97gl00504

Minobe, S. (2000). Spatio-temporal structure of the pentadecadal variability over the North Pacific. *Prog. Oceanogr.* 47, 381–408. doi:10.1016/s0079-6611(00)00042-2

Mochizukia, T., Ishii, M., Kimoto, M., Chikamoto, Y., Watanabe, M., Nozawa, T., et al. (2010). Pacific decadal oscillation hindcasts relevant to near-term climate prediction. *Proc. Natl. Acad. Sci. U. S. A.* 107, 1833–1837. doi:10.1073/pnas.0906531107

Newman, M., Compo, G. P., and Alexander, M. A. (2003). ENSO-Forced variability of the pacific decadal oscillation. *J. Clim.* 16, 3853–3857. doi:10.1175/1520-0442(2003)016<3853:evotpd>2.0.co;2

Newman, M., Alexander, M. A., Ault, T. R., Cobb, K. M., Deser, C., Di Lorenzo, E., et al. (2016). The pacific decadal oscillation, revisited. *J. Clim.* 29, 4399–4427. doi:10.1175/jcli-d-15-0508.1

Nitta, T., and Yamada, S. (1989). Recent warming of tropical sea surface temperature and its relationship to the Northern Hemisphere circulation. *J. Meteorological Soc. Jpn.* 67, 375–383. doi:10.2151/jmsj1965.67.3_375

Overland, J. E., Adams, J. M., and Bond, N. A. (1999). Decadal variability of the aleutian low and its relation to high-latitude circulation. *J. Climate* 12, 1542–1548. doi:10.1175/1520-0442(1999)012<1542:DVOTAL>2.0.CO;2

Overland, J., Rodionov, S., Minobe, S., and Bond, N. (2008). North Pacific regime shifts: Definitions, issues and recent transitions. *Prog. Oceanogr.* 77, 92–102. doi:10.1016/j.pocean.2008.03.016

Power, S., Casey, T., Folland, C., Colman, A., and Mehta, V. (1999). Interdecadal modulation of the impact of ENSO on Australia. *Clim. Dyn.* 15, 319–324. doi:10.1007/s003820050284

Pu, X., Chen, Q., Zhong, Q., Ding, R., and Liu, T. (2018). Influence of the North Pacific Victoria mode on Western North Pacific tropical cyclone Genesis. *Clim. Dyn.* 52, 245–256. doi:10.1007/s00382-018-4129-z

Qin, M., Li, D., Dai, A., Hua, W., and Ma, H. (2018). The influence of the Pacific Decadal Oscillation on North Central China precipitation during boreal autumn. *Int. J. Climatol.* 38, e821–e831. doi:10.1002/joc.5410

Rayner, N. A., Parker, D. E., Horton, E. B., Folland, C. K., Alexander, L. V., Rowell, D. P., et al. (2003). Global analyses of sea surface temperature, sea ice, and night marine air temperature since the late nineteenth century. *J. Geophys. Res.* 108, D14. 4407. doi:10.1029/2002jd002670

Reid, P. C., Hari, R. E., Beaugrand, G., Livingstone, D. M., Marty, C., Straile, D., et al. (2016). Global impacts of the 1980s regime shift. *Glob. Change Biol.* 22, 682–703. doi:10.1111/gcb.13106

Rodionov, S. N. (2004). A sequential algorithm for testing climate regime shifts. *Geophys. Res. Lett.* 31, L09204. doi:10.1029/2004gl019448

Schneider, N., Miller, A. J., and Pierce, D. W. (2002). Anatomy of NorthNorth Pacific decadal variability. *J. Clim.* 15, 586–605. doi:10.1175/1520-0442(2002)015<0586:aonpdv>2.0.co;2

Schneider, N., and Miller, A. (2001). Predicting Western North Pacific ocean climate. *J. Clim.* 14, 3997–4002. doi:10.1175/1520-0442(2001)014<3997:pwnpoc>2.0.co;2

Song, S., Yeh, S., and Park, J. (2020). Dissimilar characteristics associated with the 1976/1977 and 1998/1999 climate regime shifts in the North Pacific. *Theor. Appl. Climatol.* 142, 1463–1470. doi:10.1007/s00704-020-03378-y

Trenberth, K. E., Branstator, G. W., Karoly, D., Kumar, A., Lau, N.-C., and Ropelewski, C. (1998). Progress during TOGA in understanding and modeling global teleconnections associated with tropical sea surface temperatures. *J. Geophys. Res.* 103, 14291–14324. doi:10.1029/97jc01444

Trenberth, K. E., and Hurrell, J. W. (1994). Decadal atmosphere-ocean variations in the Pacific. *Clim. Dyn.* 9, 303–319. doi:10.1007/bf00204745

Trenberth, K. E. (1990). Recent observed interdecadal climate changes in the Northern Hemisphere. *Bull. Amer. Meteor. Soc.* 71, 988–993. doi:10.1175/1520-0477(1990)071<0988:roicci>2.0.co;2

Trenberth, K. E. (2015). Has there been a hiatus? *Science* 349, 691–692. doi:10.1126/science.aac9225

Wang, B., and Ding, Q. (2006). Changes in global monsoon precipitation over the past 56 years. *Geophys. Res. Lett.* 33, L06711. doi:10.1029/2005GL025347

Wang, B., Liu, J., Kim, H., Webster, P., and Yim, S. (2012). Recent Change of the global monsoon precipitation (1979-2008). *Clim. Dyn.* 39, 1123–1135. doi:10.1007/s00382-011-1266-z

Wang, M., Gu, Q., Jia, X., and Ge, J. (2019). An assessment of the impact of Pacific Decadal Oscillation on autumn droughts in North China based on the Palmer drought severity index. *Int. J. Climatol.* 39, 5338–5350. doi:10.1002/joc.6158

Wei, W., Yan, Z., and Li, Z. (2021). Influence of pacific decadal oscillation on global precipitation extremes. *Environ. Res. Lett.* 16, 044031. doi:10.1088/1748-9326/abed7c

Wen, T., Chen, Q., Li, J., Ding, R., Tseng, Y.-H., Hou, Z., et al. (2020). Influence of the North Pacific Victoria mode on the madden–julian oscillation. *Front. Earth Sci.* 8, 584001. doi:10.3389/feart.2020.584001

Wu, L. X., Dong, E. L., and Zheng, Y. L. (2005). The 1976/77 North Pacific climate regime shift: The role of subtropical ocean adjustment and coupled ocean-atmosphere feedbacks. *J. Clim.* 18, 5125–5140. doi:10.1175/jcli3583.1

Wu, X., and Mao, J. (2017). Interdecadal variability of early summer monsoon rainfall over South China in association with the Pacific Decadal Oscillation. *Int. J. Climatol.* 37, 706–721. doi:10.1002/joc.4734

Xiao, D., and Li, J. (2007a). Main decadal abrupt changes and decadal modes in the global sea surface temperature field (in Chinese with English figure captions). *Chin. J. Atmos. Sci.* 31, 839–854. doi:10.3878/j.issn.1006-9895.2007.05.08

Xiao, D., and Li, J. (2007b). Spatial and temporal characteristics of the decadal abrupt changes of global atmosphere-ocean system in the 1970s. *J. Geophys. Res.* 112, D24S22. doi:10.1029/2007jd008956

Xiao, D., and Li, J. (2011). Mechanism of stratospheric decadal abrupt cooling in the early 1990s as influenced by the Pinatubo eruption. *Chin. Sci. Bull.* 56, 772–780. doi:10.1007/s11434-010-4287-9

Xiao, D., and Ren, H.-L. (2021). Interdecadal changes in synoptic transient eddy activity over the Northeast Pacific and their role in tropospheric Arctic amplification. *Clim. Dyn.* 57, 993–1008. doi:10.1007/s00382-021-05752-6

Xiao, D., Li, J., and Zhao, P. (2012). Four-dimensional structures and physical process of the decadal abrupt changes of the northern extratropical ocean-atmosphere system in the 1980s. *Int. J. Climatol.* 31, 983–994. doi:10.1002/joc.2326

Xiao, D., Zhao, P., and Ren, H.-L. (2021). Climatic factors contributing to interannual and interdecadal variations in the meridional displacement of the East Asian jet stream in boreal winter. *Atmos. Res.* 264, 105864. doi:10.1016/j.atmosres.2021.105864

Xu, M., Xu, H., Ma, J., and Deng, J. (2021). Impact of pacific decadal oscillation on interannual relationship between El Niño and SouthSouth China Sea summer monsoon onset. *Int. J. Climatol.* 42, 1–15. doi:10.1002/joc.7388

Yao, J., Xiao, L., Gou, M., Li, C., Lian, E., and Yang, S. (2018). Pacific decadal oscillation impact on East China precipitation and its imprint in new geological documents. *Sci. China Earth Sci.* 61, 473–482. doi:10.1007/s11430-016-9146-2

Yeh, S., Kang, Y., Noh, Y., and Miller, A. J. (2011). The North pacific climate transitions of the winters of 1976/77 and 1988/89. *J. Clim.* 24, 1170–1183. doi:10.1175/2010jcli3325.1

You, J., Jian, M., Gao, S., and Cai, J. (2021). Interdecadal change of the winter-spring tropospheric temperature over asia and its impact on the SouthSouth China Sea summer monsoon onset. *Front. Earth Sci.* 8, 599447. doi:10.3389/feart.2020.599447

Zhang, Y., Wallace, J. M., and Battisti, D. S. (1997). ENSO-Like interdecadal variability: 1900–93. *J. Clim.* 10, 1004–1020. doi:10.1175/1520-0442(1997)010<1004:eliv>2.0.co;2

Zhang, C., Li, S., Luo, F., and Huang, Z. (2019). The global warming hiatus has faded away: An analysis of 2014-2016 global surface air temperatures. *Int. J. Climatol.* 39, 4853–4868. doi:10.1002/joc.6114

Zhu, Y., Wang, H., Ma, J., Wang, T., and Sun, J. (2015). Contribution of the phase transition of Pacific Decadal Oscillation to the late 1990s' shift in East China summer rainfall. *J. Geophys. Res. Atmos.* 120, 8817–8827. doi:10.1002/2015jd023545

Zou, Q., Ding, R., Li, J., Tseng, Y.-H., Hou, Z., Wen, T., et al. (2020). Is the North Pacific Victoria mode a predictor of winter rainfall over SouthSouth China? *J. Clim.* 33, 8833–8847. doi:10.1175/jcli-d-19-0789.1